Hindawi
Geofluids
Volume 2022, Article ID 3910721, 18 pages
https://doi.org/10.1155/2022/3910721

Research Article

Investigating Reliability of Duimenshan High Rock Slope in Gejiu, Yunnan Province Based on the Monte Carlo Method

A. Fa-You,[1,2] **Wan-cheng Pan**,[1] **Wen-ping Wu**,[3,4] **and Shi-qun Yan**[1]

[1]*Faculty of Land Resource Engineering, Kunming University of Science and Technology, Kunming Yunnan 650093, China*
[2]*Key Laboratory of Geohazard Forecast and Geoecological Restoration in Plateau Mountainous Area, Ministry of Natural Resources of the People's Republic of China, Kunming Yunnan 650000, China*
[3]*China Ordnance Industry Survey and Geotechnical Institute Co., Ltd., China*
[4]*Beijing China Ordnance Industry Geotechnical Engineering Co., Ltd., China*

Correspondence should be addressed to A. Fa-You; afayou@163.com

Received 27 July 2022; Revised 22 September 2022; Accepted 27 September 2022; Published 17 October 2022

Academic Editor: Hailing Kong

A slope is a complex engineering geological body that contains many uncertainties. In the present study, the high rock slope of Duimenshan in Gejiu, China is taken as the research object, and the Monte Carlo method is used to perform the analyses. Firstly, based on a large number of rock mass discontinuities, the Fuzzy C-Means (FCM) clustering algorithm is used to determine the dominant discontinuities. Secondly, the affecting parameters of the rock mass such as cohesion, internal friction angle, horizontal seismic acceleration coefficient, and water-filled depth coefficient are taken as random variables, and the failure probability of the slope and the failure index corresponding to different slope heights and slopes are obtained as the output parameter. The obtained results show that the target reliability index of the slope in a certain range of the slope height is far from the safety value, indicating that the slope is unstable, and the combination of slope height and slope angle affects the reliability of the slope. More specifically, as the slope height and angle increase, the number of samples with a stability coefficient of less than 1 increases, thereby increasing the failure probability of the slope indicating that the slope is stable. It is found that unless the slope height is small, it is the main factor of stability. However, when the slope height exceeds 33 m, the effect of the slope inclination on the stability increases gradually.

1. Introduction

Slope Engineering is a complex engineering geological body that deals with many complex problems such as uncertainties of physical and mechanical parameters of rock and soil mass and the space-time variability, the complexity, diversity, and randomness of external factors such as rainstorm [1], earthquake [2], groundwater [3], load [4], artificial blasting [5], and karstification [6]. Accordingly, stability analysis of slope engineering is a very challenging task. Studies show that relying only on a single index or analysis method may lead to inaccurate results that cannot be used in engineering applications [7, 8].

The rigid body limit equilibrium method, which is mainly used in slope stability quantitative analysis, is based on the factor of safety method and cannot objectively consider uncertainty and variability of rock mass parameters. In this method, ignoring the effect of these factors may lead to inaccurate and inconsistent results, thereby increasing potential security risks. Therefore, it is of significant importance to introduce the reliability analysis method into slope engineering [9–11]. Compared with nonphysical assumptions and theories in mathematical analysis methods, numerous physical parameters, including the structural characteristics of the slope, parameters of the rock mass discontinuity, rainfall, earthquake, and groundwater are regarded as random variables, and then the random variables are expressed by rational functions. Consequently, this method can be effectively applied to solve the internal uncertainty and randomness of rock and soil slope. Accordingly, the limit equilibrium method can be applied to obtain more comprehensive and objective results.

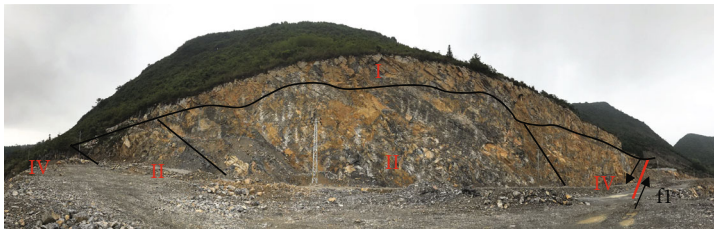

Figure 1: Division of slope landform and rock group.

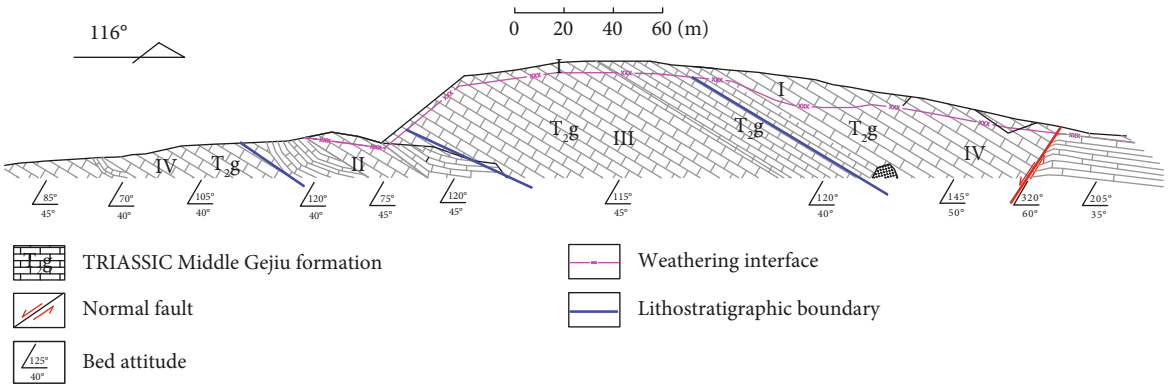

Figure 2: Elevation diagram of slope in the study area.

Table 1: Shear strength index of the rock mass.

Rock group	Density ρ(g/cm^3)	Cohesive force c/MPa	Angle of internal friction φ/∘	Modulus of deformation Em (MPa)
(1.1) strong weathered medium-thick limestone with relatively weak rock groups	2.73	0.06	13.28	1.0
(1.2) strong weathered thin limestone with relatively weak rock groups	2.73	0.05	11.91	0.9
(2) Thin bedded limestone with hard rock groups	2.75	0.18	28	3.65
(3) Medium-thick bedded limestone hard rock groups	2.75	0.18	29	4.1
(4) Middle-thick bedded limestone, which is harder than hard rock groups	2.75	0.18	28	4.1

Figure 3: F1 fault crossing the slope.

Currently, the common slope reliability analysis methods are the Monte Carlo method [12–17], response surface method (RSM) [18–20], Latin hypercube sampling (LHS) multidimensional stratified sampling method [21–24], and first-order second-moment method (FOSM) [25–28]. In this regard, the Monte Carlo method is widely used in financial engineering, biomedicine, economics, computational physics, and geotechnical engineering. Since the convergence rate of this method is not restricted by the dimension of random variables and the function complexity, it can be applied to quickly and accurately solve the problem and determine the simulation error. It can be seen that Monte Carlo method has many advantages, and it can be seen from previous studies that applied research has made more achievements. But in the field of slope engineering, how to introduce the information of structural plane and other random variables into the application of this method more accurately will become an important link whether the

Table 2: Rock mass discontinuities.

Measuring point	Attitude		Description of joint geometry			Filling feature			Number and spacing of groups		Face type
	Dip angle (°)	Direction of tilt(°)	Extensibility	Opening degree	Surface form	Material composition	Size composition	Degree of filling%	Group number	Spacing (cm)	
1	55	85	Through	Slightly open	Smoothed	Calcareous	Fine grain	5	3	30~40	Bedding plane
	70	320	Half through	Close up	Coarseness	Calcareous	Fine grain	2	10	10~20	Joint
	65	200	Nonthrough	Slightly open	Smoothed	Argillaceous	Fine grain	80	3	30~40	Joint
2	40	70	Through	Slightly open	Smoothed	Calcareous	Fine grain	0	4	20~30	Bedding plane
	80	245	Nonthrough	Open	Smoothed	Calcareous	Fine grain	2	2	40~50	Joint
	42	300	Nonthrough	Slightly open	Smoothed	Calcareous	Fine grain	5	2	40~50	Joint
3	40	120	Through	Slightly open	Smoothed	Calcareous	Fine grain	0	4	20~30	Bedding plane
	45	270	Half through	Close up	Coarseness	Calcareous	Fine grain	10	5	10~20	Joint
	85	230	Half through	Slightly open	Smoothed	Calcareous	Fine grain	5	6	10~20	Joint
4	45	75	Through	Slightly open	Smoothed	Argillaceous	Fine grain	80	12	0 ~ 10	Bedding plane
	83	280	Nonthrough	Slightly open	Smoothed	Argillaceous	Fine grain	85	3	30~40	Joint
	84	215	Nonthrough	Open	Smoothed	Argillaceous	Fine grain	80	4	20~30	Joint
5	45	125	Through	Slightly open	Coarseness	Argillaceous	Fine grain	80	1	>50	Bedding plane
	50	290	Half through	Slightly open	Smoothed	Argillaceous	Fine grain	85	12	0 ~ 10	Joint
	84	35	Nonthrough	Slightly open	Smoothed	Argillaceous	Fine grain	80	1	>50	Joint
6	45	75	Through	Close up	Smoothed	Calcareous	Fine grain	10	8	10~20	Joint
	75	275	Nonthrough	Close up	Coarseness	Argillaceous	Fine grain	0	3	30~40	Joint
	55	170	Half through	Slightly open	Smoothed	Calcareous	Fine grain	5	3	30~40	Joint

Table 2: Continued.

Measuring point	Attitude		Description of joint geometry			Filling feature			Number and spacing of groups		Face type
	Dip angle (°)	Direction of tilt(°)	Extensibility	Opening degree	Surface form	Material composition	Size composition	Degree of filling%	Group number	Spacing (cm)	
7	45	115	Through	Slightly open	Smoothed	Calcareous	Fine grain	0	3	30~40	Bedding plane
	70	210	Nonthrough	Slightly open	Smoothed	Calcareous	Fine grain	5	3	30~40	Joint
	75	180	Half through	Close up	Coarseness	Calcareous	Fine grain	2	6	10~20	Joint
	32	305	Nonthrough	Close up	Smoothed	Calcareous	Fine grain	2	12	0 ~ 10	Joint
8	40	120	Through	Slightly open	Smoothed	Calcareous	Fine grain	2	5	10~20	Bedding plane
	55	295	Nonthrough	Slightly open	Smoothed	Calcareous	Fine grain	2	4	20~30	Joint
	80	190	Half through	Slightly open	Smoothed	Calcareous	Fine grain	5	3	30~40	Joint
9	25	115	Through	Slightly open	Smoothed	Calcareous	Fine grain	5	3	30~40	Bedding plane
	80	230	Half through	Slightly open	Smoothed	Calcareous	Fine grain	0	2	40~50	Joint
	85	35	Nonthrough	Close up	Smoothed	Calcareous	Fine grain	10	3	30~40	Joint
10	15	160	Through	Close up	Smoothed	Calcareous	Fine grain	11	2	40~50	Bedding plane
	84	350	Nonthrough	Slightly open	Smoothed	Calcareous	Fine grain	5	2	40~50	Joint
	85	210	Half through	Slightly open	Smoothed	Calcareous	Fine grain	0	2	40~50	Joint
11	35	110	Through	Close up	Smoothed	Calcareous	Fine grain	10	3	30~40	Bedding plane
	55	220	Nonthrough	Slightly open	Smoothed	Calcareous	Fine grain	0	3	30~40	Joint
	84	320	Half through	Close up	Smoothed	Calcareous	Fine grain	15	3	30~40	Joint

Table 2: Continued.

Measuring point	Attitude		Description of joint geometry			Filling feature			Number and spacing of groups		Face type
	Dip angle (°)	Direction of tilt(°)	Extensibility	Opening degree	Surface form	Material composition	Size composition	Degree of filling%	Group number	Spacing (cm)	
12	45	145	Through	Slightly open	Smoothed	Calcareous	Fine grain	5	3	30~40	Bedding plane
	45	275	Half through	Slightly open	Coarseness	Calcareous	Fine grain	2	3	30~40	Joint
	85	210	Nonthrough	Open	Smoothed	Calcareous	Fine grain	5	3	30~40	Joint
	60	320	Through	Open	Coarseness	Argillaceous	Fine grain	95	1	—	Fault
13	45	205	Through	Slightly open	Smoothed	Argillaceous	Fine grain	85	3	30~40	Bedding plane
	70	175	Nonthrough	Slightly open	Smoothed	Argillaceous	Fine grain	85	4	20~30	Joint
	55	155	Half through	Slightly open	Smoothed	Argillaceous	Fine grain	90	3	30~40	Joint

analysis method is reliable or not; few studies have done sourcing circumstances analysis of random variables. Therefore, in this study, the high rock slope in the construction site of the heavy metal pollution treatment demonstration zone in the Gejiu area of Yunnan Province was selected as the research object, and the dominant structural planes of the slope were determined by using the Fuzzy C-Means (FCM) clustering algorithm, and then the reliability of the high rock slope was analyzed by using the Monte Carlo method; it provides the basis for the permanent treatment of the slope and the safety guarantee for the construction and operation of the demonstration test area.

2. Geological Condition of the Slope

2.1. Topography. The landform of the slope area belongs to the karst fault block of high and middle mountains with scarce vegetation and up-steep and down-gentle characteristics. The natural slope at the top of the excavation slope is in the range of 5°-10°. The slope is steeper near the ridge, and the maximum slope is 35°. The slope is located in the west section of the north side of the proposed site. The total length and the maximum height in the middle and two sides of the excavated slope are 460 m, 50 m, and 5-10 m, respectively. Moreover, the excavation slope is in the range of 80°-85°.

2.2. Formation Lithology. Based on the engineering exploration, the main strata lithology distributed in the study area are Quaternary Plant Layer (Q^{pd}), quaternary slope eluvium (Q^{dl+el}) that contains gravelly silty clay, and underlying bedrock strata (T_2g^2) that contain limestone of the Middle Triassic Gejiu formation. According to the distribution of rock mass, borehole data, and geological data of the slope, the engineering geological rock group of the slope can be divided into the following four main categories and two subcategories: (1) strong weathered limestone with relatively weak rock groups; (1.1) strong weathered medium-thick limestone with relatively weak rock groups; (1.2) strong weathered thin limestone with relatively weak rock groups; (2) thin bedded limestone hard rock group; (3) medium-thick bedded limestone hard rock group; and (4) middle-thick bedded limestone, which is harder than hard rock groups. Moreover, Figures 1 and 2 illustrate that the slope can be divided into five areas according to the engineering geological rock group. Table 1 shows the shear strength of each rock group.

2.3. Geological Structures. The study area is located in the south of Gejiu. The main regional affecting faults include the Red River deep fault in the south and the east-west Kaofang fault in the west, which is 1.5 km away. Other regional faults are relatively far from the study area and can be ignored. Figure 3 shows that there is a normal fault (f1) in the southeast section of the slope with an attitude of 60°∠60°. The strike of the fault is nearly perpendicular to the strike of the slope. Moreover, the traction structure is developed in the rock strata of the two sides of the fault, the rock mass is broken, and the fault fracture zone is obvious.

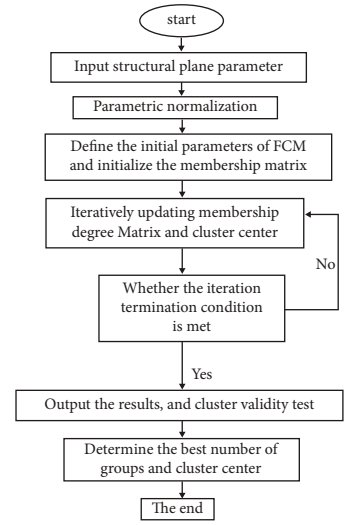

Figure 4: The flow diagram of the FCM algorithm.

Figure 2 shows the elevation diagram of the slope indicating that the whole direction of strata is to the northwest, the direction of tilt is to the southeast, and the slope structure is of oblique type. The dip angle of rock strata varies greatly, which may be attributed to faults and local compressions. In the northwest section of the slope, the bed attitude is 40°-45°∠70°-120°. The attitude of the rock layer in the middle section of the slope is relatively stable, and the bed attitude is 40°-45°∠115°-145°. The southeast section of the slope is located in the footwall of the fault, and the traction deformation of the local rock strata changes the slope structure to a consequent type slope, which is detrimental to the slope stability.

2.4. Hydrogeological Conditions. According to the difference between strata and lithology and the form, space, and hydraulic characteristics of the groundwater, the groundwater in the study area can be mainly divided into two categories, including pore water and karst water. It is worth noting that there is no underground water in the borehole and no underground spring in the vicinity.

3. Determination of Dominant Structural Plane Based on the Fuzzy C-Means (FCM) Clustering Algorithm

According to the performed field survey, the high rock slope is 480 m long. The detailed survey line method is used to investigate the structural plane of rock mass with a length of 13.00 m and 164 joints. The main characteristics of the rock mass are presented in Table 2.

Dunn [29] proposed the Fuzzy C-Means (FCM) algorithm as a clustering scheme based on an objective function. The core idea of this algorithm is to find the minimum objective function by updating the clustering center and

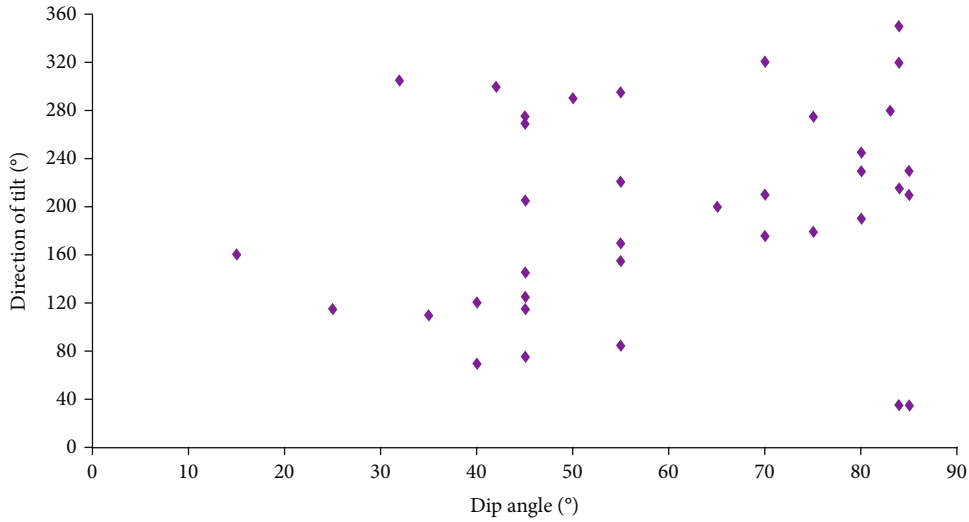

Figure 5: Distribution of discontinuity attitude.

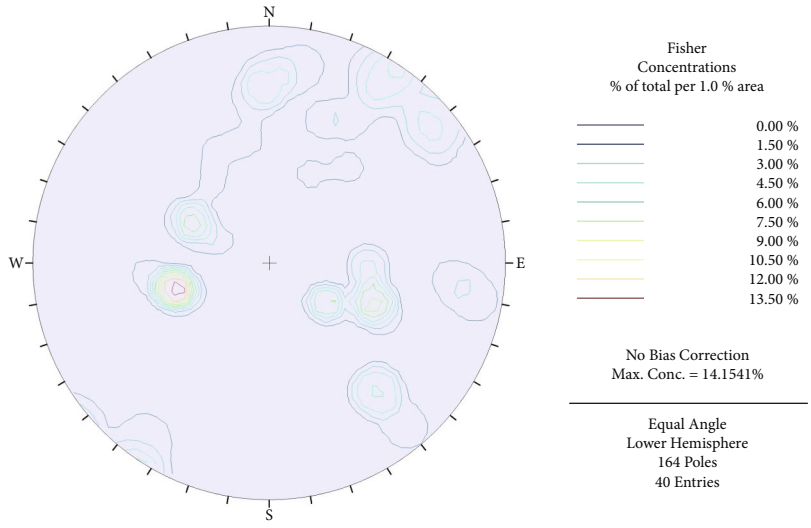

Figure 6: Density contours of structure plane pole.

Table 3: Validity test results.

Group number	2	3	4	5	6	7	8	9
Vs	0.241	0.168	0.173	0.202	0.208	0.211	0.210	0.251

membership function. This algorithm has a simple design and wide applications that are widely used as an effective fuzzy cluster analysis method.

The main steps of the FCM algorithm can be summarized as follows: define and normalize the parameters of the structural plane in the computer program, define the initial conditions and set an appropriate number of clusters K in the range of 2~9, and set the convergence precision, the number of iterations t, and the fuzzy weighting index m. Then, compare the difference of cluster centers under different grouping conditions to check whether the number of iterations has reached t or Max $\|U^t - U^{t-1}\| < \mu$. The values of the validity test of silhouette under different grouping are analyzed to determine the best grouping number and cluster center. Figure 4 illustrates the flow diagram of the FCM algorithm.

Figures 5 and 6 show the plane diagram of the occurrence distribution of the structural plane and the density diagram of the structural plane poles of the slope in the original state. It should be indicated that it is an enormous challenge

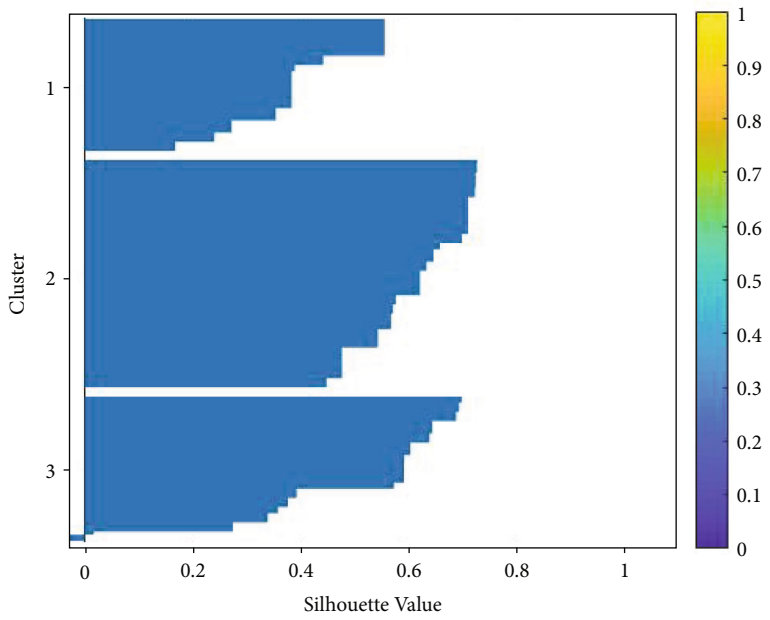

(a) Three-group classification

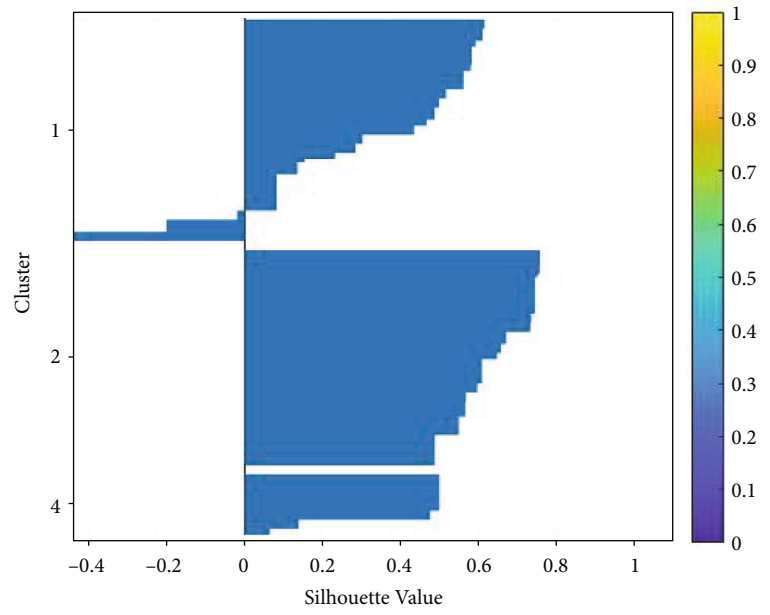

(b) Four-group classification

Figure 7: Continued.

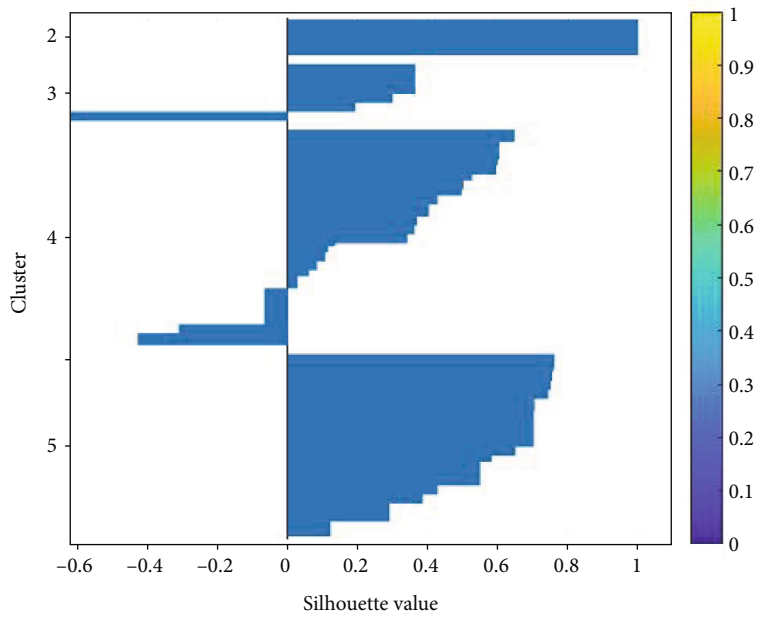

(c) Five-group classification

Figure 7: Diagrams of clustering validity grouping effect.

Table 4: Results of the FCM method for structural plane grouping.

Categories	Direction of tilt/(°)	Dip angle/(°)	Quantitative value of surface morphology	Quantitative value of extensibility	Quantitative value of opening degree	Group number
1	246.4	47.9	0.160	0.731	0.414	43
2	166.2	50.2	0.196	0.684	0.365	74
3	211.7	74.7	0.932	0.577	0.399	47

to classify and analyze these poles using conventional methods. Based on the mathematical statistics function of the FCM algorithm, a cluster analysis is carried out on the five parameters of 164 groups of structural plane parameters. These parameters are dip angle, direction of tilt, ductility, opening degree, and roughness. The number of clusters is 2~9, and the total number of iterations is set to 800.

The cluster validity test value Vs (Table 3) and the cluster validity grouping effect diagram of 3~5 groups (Figure 7) were obtained through iterative calculations. It is observed that when the dominant structure plane is divided into 4 and 5 groups, a negative number of Vs appears, which is not consistent with the interval of the objective function. Moreover, when there are 3 groups, Vs reach the minimum value and negative numbers disappear. Accordingly, the optimal grouping number of dominant discontinuities in the rock mass is 3 groups.

After determining the optimal grouping of dominant discontinuities using the FCM clustering algorithm, the final data in a rock mass can be obtained according to the radian transformation of the data of the cluster center (Table 4). Then DIPS software is utilized to perform the FCM algorithm, and the obtained contour of the structural plane pole is presented in Figure 8. Compared with Figure 6, the distribution of the structural plane of rock mass after clustering analysis is more clear, and the desired result is achieved.

4. Determination of Objective Reliability of the Slope

The objective reliability (also called reliability design) and the acceptable risk of slope design can meet the requirements of slope engineering design. So far, no uniform criterion of slope reliability has been proposed in this regard. To resolve this shortcoming, the calibration method and the analogy method are applied to determine the target reliability index. It is intended to refer to the current standards for reliability indicators, analyze the key points, and refer to the reliable design codes such as construction slope, railway, highway, water conservancy, and hydropower slope. The calibration method not only inherits the current design standard but also fully reflects the long-term practical experience of experts in engineering construction. Therefore, this method has been widely adopted worldwide.

4.1. Slope Service Life. According to "The unified standard for reliability design of engineering structures" (GB50153-2008), designing the service life is the basic prerequisite to

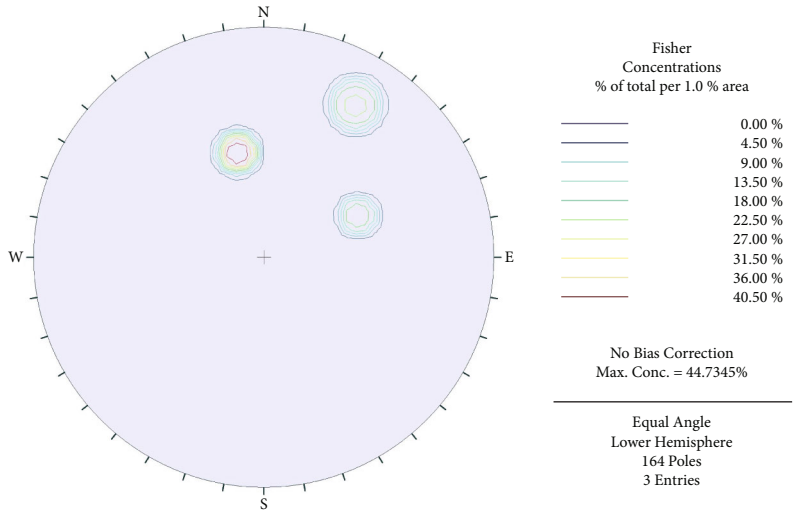

Figure 8: The pole contour of the dominant structural plane based on the FCM method.

Table 5: Structural safety rating table.

Safety rating	Examples
First degree	Important structures such as large-scale public buildings
Second degree	Ordinary residential and office buildings and other general structure
Third degree	Minor structures such as small or temporary storage buildings

Table 6: Design life of building structures.

Design life (years)	Examples
5	Temporary building structure
25	Easily replaceable structural member
50	Ordinary houses and structures
100	Landmarks and important buildings

satisfy the reliability of engineering structures. Therefore, it is necessary to determine the design life (service life) before determining the target reliability of slope engineering.

According to the "The technical code for Building Slope Engineering" (GB50513-2013), the design service life of a building slope should not be less than the design service life of a protected building (structure). Based on the safety grade table (Table 5) and the design life table (Table 6) of "Building structures specified in the unified standard for reliability design of building structures" (GB50068-2018), the proposed buildings in the slope project (Table 7) and the service life of the buildings in this area are determined to be 50 years.

Table 8 shows the service life table of slope engineering indicating that the service life of slope should be higher than 50 years.

4.2. Slope Safety Grade. The classification of slope safety is mainly affected by the slope height and hazard degree, which can be obtained according to "Unified Standard for Reliability Design of Engineering Structures" (GB50153-2008), "Technical Code for Building Slope Engineering" (GB50513-2008), and "Slope Design Code for Water Resources and Hydropower Projects" (SL386-2007). In this regard, the obtained results are presented in Tables 9 and 10.

4.3. Target Reliability of the Slope. Currently, there is no unified standard for the reliability design of slope engineering. However, the studied slope is of building type slope. Therefore, according to "Unified Standard for Reliability Design of Building Structures" (GB50068-2018), "Unified Standard for Reliability Design of Engineering Structures" (GB50153-2008), and the conventional standards about reliability in railway, highway, water conservancy, hydropower, and port engineering, an inductive analysis can be carried out [30]. In this regard, the obtained results are presented in Tables 11 and 12.

Since the studied slope is a high rock slope with a height of more than 30 m and referred to item 3.2.5 of "Unified Standard for Reliability Design of Engineering Structures" (GB50153-2008) stipulates that "the value of reliability index should be 0.5 for every grade difference of safety level"; the target reliability index of the slope is determined in Table 13.

5. Reliability Analysis of Slope Based on MCS

Considering uncertainty and complexity of affecting factors on the stability of slope engineering, the Monte Carlo

Table 7: List of proposed buildings.

Name of building (structure)	Number of plies	Height (m)	Building grade	Structure type	Building materials
2000 t/tin-copper sulfide ore dressing plant	One	12.3	Two	Bent	Reinforced concrete
1000 t/tin oxide concentrator	One	9.9	Two	Bent	Reinforced concrete
Seven 500 t/tin-copper sulfide ore dressing plants	One	6.6	Two	Bent	Reinforced concrete
Tin concentration workshop	One	9.5	Two	Bent	Reinforced concrete

Table 8: Reasonable service life of slope engineering.

Design service life of buildings (structures) (years)	Safety grade of buildings (structures)	Example	Length of service (years)
100	First degree	Landmark buildings and important buildings	>100
50	Second degree	Ordinary houses and structures	>50
25	Third degree	Or small temporary storage buildings.	>25

Table 9: Safety grade of slope engineering.

Slope type		Consequence of destruction	Height of slope h (m)	Security level/phase
Rock slope	Rock mass type i or ii	Very serious	$h \le 30$	First degree
		Serious		Second degree
		Not serious		Third degree
	Rock mass type is iii or iv	Very serious	$30 \ge h > 15$	First degree
		Serious		Second degree
		Very serious	$h \le 15$	First degree
		Serious		Second degree
		Not serious		Third degree

simulation (MCS) method is applied to analyze the reliability of slope engineering. In this method, the influence of many uncertain factors is considered in the calculations. The slope reliability which determines whether the slope function can meet the design and use requirements within a certain period of time, that the larger the reliability index, the lower the slope failure probability.

The basic idea of the applied reliability analysis method can be summarized as follows: based on the Monte Carlo method, the slope height h, slope angle β, cohesion c, internal friction angle φ, and the horizontal seismic acceleration coefficient $\boldsymbol{\alpha}$ of rock slope are taken as random variables, and then the stability coefficient F_s corresponding to n random samples is calculated by solving the problem in MATLAB environment. Further statistical analysis of the number of failure samples in random samples (i.e., the number of samples with $F_s < 1$) is carried out, and then the target failure probability of slope and the statistical characteristics of rock mass parameters are calculated. Finally, the slope reliability is evaluated [31–33].

5.1. Specific Implementation Steps. Figure 9 shows the flowchart of the reliability analysis of the rock slope using the Monte Carlo method.

Similar to Hoek [34] and Wang et al. [35], it is assumed that the rock slope is composed of a single unstable block. In other words, the failure mode is simplified as a planar two-dimensional rock mass sliding failure. Figure 10 shows the slope calculation model, and the mathematical expression is presented.

$$F_S = \frac{\mathrm{cA} + [W(\cos\alpha - \boldsymbol{\alpha}\sin\alpha) - U - V\sin\alpha]\tan\varphi}{W(\boldsymbol{\alpha}\cos\alpha + \sin\alpha) + V\cos\alpha}, \quad (1)$$

$$A = \frac{h - z}{\sin\alpha}, \quad (2)$$

$$W = \left\{\left[1 - \left(\frac{z}{h}\right)^2\right]\cot\alpha - \cot\beta\right\}0.5h^2\gamma, \quad (3)$$

$$U = 0.5A\gamma_w z_w, \quad (4)$$

$$V = 0.5\gamma_w {z_w}^2, \quad (5)$$

where U, A, V, and W denote the water pressure on the sliding surface, unit width area of the sliding surface, water pressure on the tensile crack surface, and the dead weight of the sliding body, respectively. Moreover, $\boldsymbol{\alpha}$ and α are horizontal seismic acceleration coefficients and slip surface dip angles, respectively. The gravity γ of the rock mass and water is 27 kN/m^3 and 10 kN/m^3, respectively, and the dip angle α of the sliding surface is 45°. Moreover,

Table 10: Grade of slope disaster.

Disaster grade		I	II	III
Economic losses	Direct	> 1 million yuan	500~1 million yuan	< 500,000 yuan
	Indirect	> 10 million yuan	100~10 million yuan	< 5 million yuan
Harmfulness		Casualties Equipment loss	Personal injury Equipment damage	No casualties. Minor loss of equipment
Overall evaluation		Very serious	Serious	Not serious

Table 11: Reliability index of the building structure.

Failure type	Security level/phase		
	First degree	Second degree	Third degree
Ductile failure	3.7	3.2	2.7
Drittle fracture	4.2	3.7	3.2

Table 12: Research results of target reliability in different engineering fields.

Security level/phase	Reliability index of different engineering fields			
	Railway	Port	Highway	Water conservancy and hydropower
I	4.2	4.0	4.7	3.7
II	3.7	3.5	4.2	3.2
III	3.2	3.0	3.7	2.7

Table 13: Target reliability index of slope.

Length of service (years)	Security level/phase		
	I	II	III
25	3.2	2.7	2.2
50	3.7	3.2	2.7
100	4.2	3.7	3.2

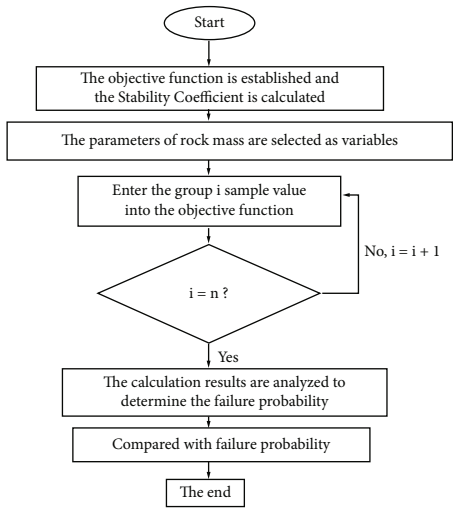

Figure 9: Flowchart of the MCS method.

z_w is the filling depth of fissure water, which is the product of z and i.

The slope is 75~85°, the height of the slope is 5~50 m, and the dip angle of the sliding surface is about 45°. Since cracks are mainly concentrated in the range of 25~50 m slope height, the simulation is focused on this range. The discrete random variables of rock mass parameters with a normal distribution include the crack depth z, cohesion c, internal friction angle φ, and horizontal seismic acceleration coefficient $\boldsymbol{\alpha}$, while the water filling depth coefficient i in the fracture follows a truncated exponential distribution. In this regard, 26 and 11 possible values are considered when the slope height and the slope angle are dispersed at 1 m and 1° equal intervals, respectively. In total, 286 cases are considered in the present study.

Based on the determination results of rock mass parameters, statistical analysis is made, and the distribution of random variable strength parameters of the slope is determined. Table 14 shows the horizontal seismic acceleration coefficient $\boldsymbol{\alpha}$ varying from 0 to 0.16, and the depth coefficient of water filling in cracks ranges from 0 to 1.

5.2. Statistical Analysis. Since the slope reliability index is in one-to-one correspondence with failure probability, the slope target failure probability P_f and the minimum sample number $n_{\min}$ required for simulation are set to 2×10^{-4} and 5.95×10^7, respectively, to ensure the calculation accuracy. The simple statistical analysis of the random variables yields the rectangular statistical Figures 11–14.

Figures 11–14 reveal that among the random variables, the number of samples of slope height h and slope angle β in each interval is constant, obeys a discrete and uniform distribution, and the number of samples in equal intervals is 7.8×10^6 and 9×10^6, respectively. However, the distribution of two random variables, internal friction angle φ and cohesion c, roughly accords with the standard normal distribution curve indicating that these variables have a normal distribution in the range of 16~37°and 120~240 kPa. Analysis results can be summarized as follows:

(1) Overall reliability analysis of the slope:

After demonstrating the rationality of the input random variables, the slope stability is calculated and analyzed in MATLAB environment. In order to improve the calculation accuracy, the slope stability was calculated and statistically analyzed three times, and the obtained results are presented in Table 15 and Figure 15

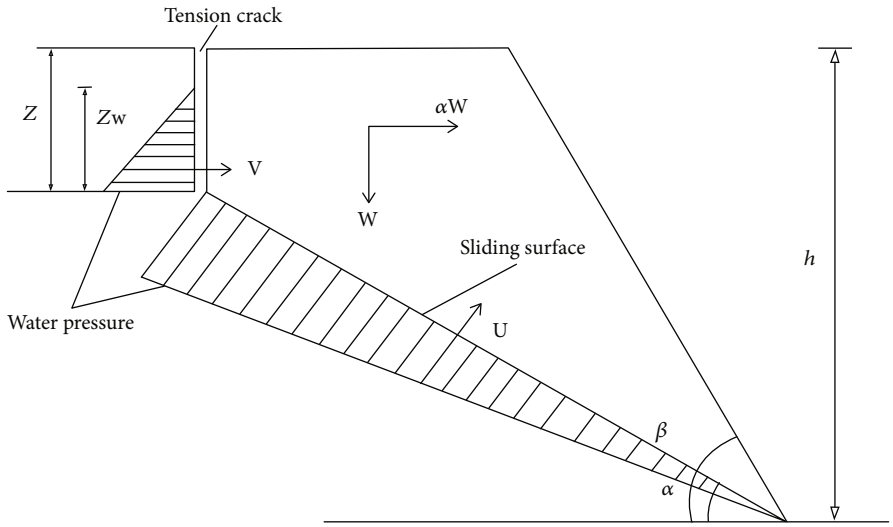

Figure 10: Slope calculation model.

Table 14: Parameter distribution of random variables.

Stochastic variable	Distribution pattern	Average/mean value	Standard deviation
Cohesion c/kPa	Normal distribution	180	15
Internal friction angle φ/(°)	Normal distribution	27.6	3
Horizontal seismic acceleration coefficient $\boldsymbol{\alpha}$	Truncated exponential distribution	0.08	—
Fracture depth z	Normal distribution	9.2	2
Coefficient of water filling depth in fissures i	Truncated exponential distribution	0.5	—
Slope height h	Discrete uniform distribution	—	—
Slope angle β	Discrete uniform distribution	—	—

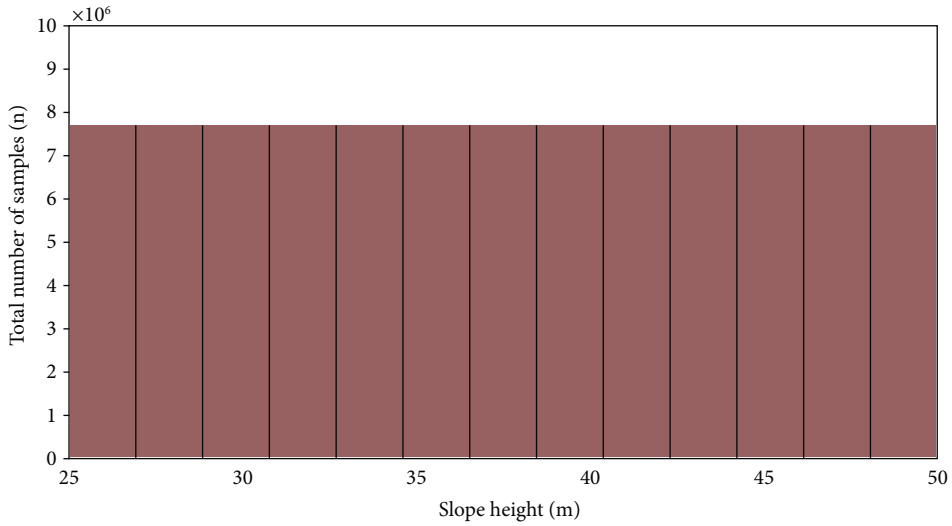

Figure 11: Statistical histogram of slope height parameters.

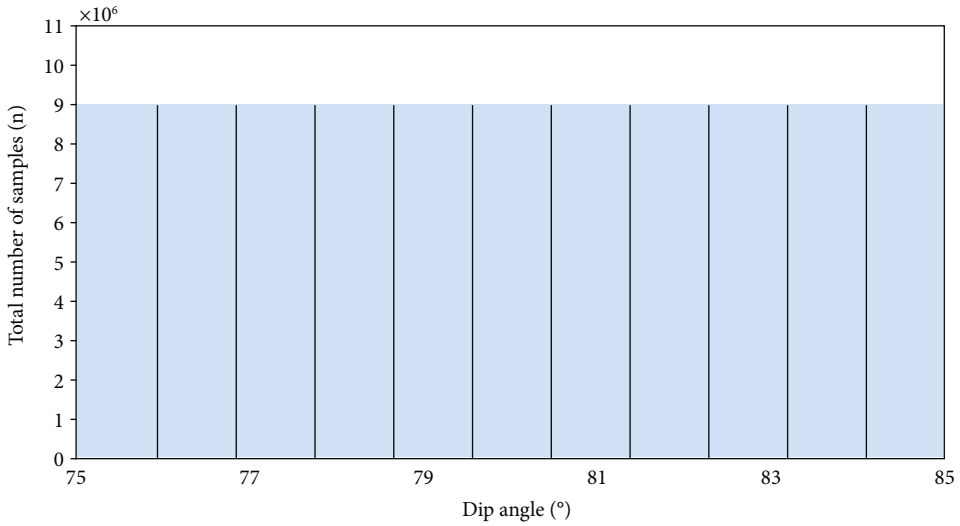

Figure 12: Statistical histogram of slope angle parameters.

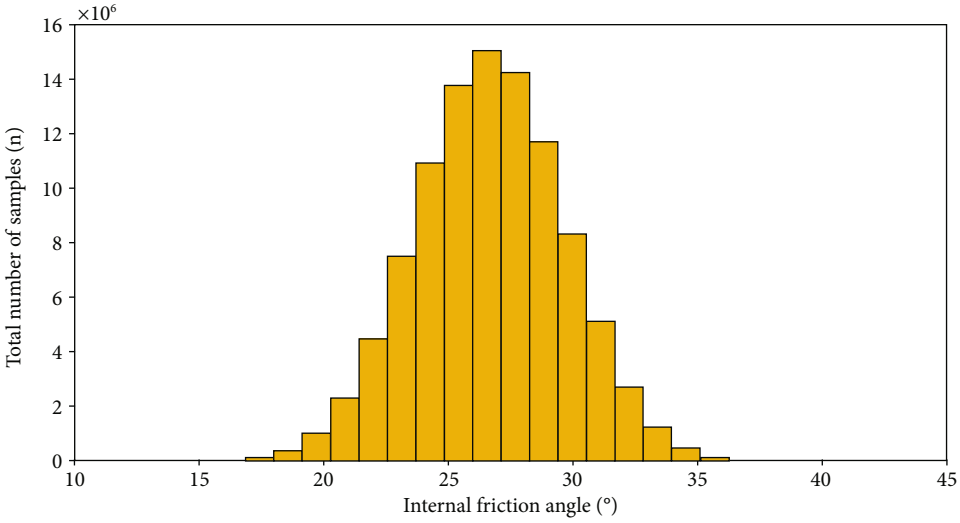

Figure 13: Statistical histogram of internal friction angle parameters.

Figure 15 shows that the stability coefficients are mostly concentrated in the interval of 0.6~2, which reflects the rationality of the input random variables and the stability of the performed calculations. Moreover, Table 15 reveals that the values of n_F and the corresponding failure probability of three groups of slope failure samples are very close, and the average value of the overall failure probability of the slope within the range of 25~50 m is 0.1477, which is much higher than the design failure probability of the slope P_f (2×10^{-4}). It is concluded that the failure probability of the slope functional structure is extremely high. To sum up, as far as the slope is concerned, the target reliability requirements of the first-class building slope cannot be achieved, and the slope is unstable so it is necessary to take timely treatment measures.

(2) Reliability analysis under different combinations of slope heights and angles:

The overall failure probability of slope $p(F)$ is obtained after the failure probability of slope corresponding to different combinations of slope height h and slope angle β $p(F\|h, \beta)$ is statistically analyzed. Figure 16 shows the statistical chart of stability safety coefficient corresponding to different combinations of slope height h and slope angle β. It is found that when the stability coefficient in a certain combination state is greater than 1, the slope is stable. Moreover, Figure 16 indicates that as the slope height and slope angle increase, more samples with a stability coefficient of less than 1 are achieved and the probability of slope failure increases, and the slope becomes unstable.

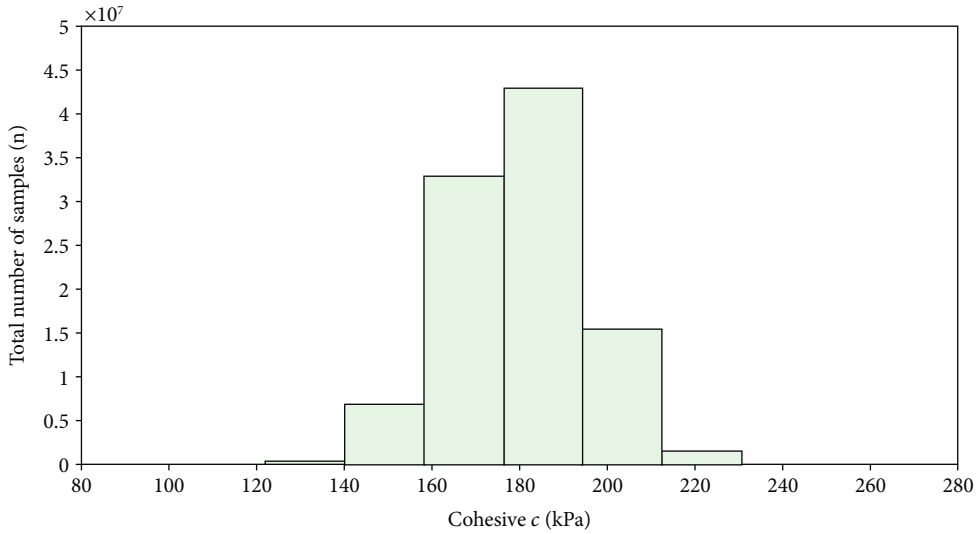

Figure 14: Statistical histogram of cohesion parameters.

Table 15: Calculation results obtained from the MCS.

MCS method	Total number of samples n	Total number of invalid samples n_F	Failure probability $p(F)$
First time	10^8	1.4762×10^7	0.1476
Second time		1.4800×10^7	0.1478
Third time		1.4765×10^7	0.1477

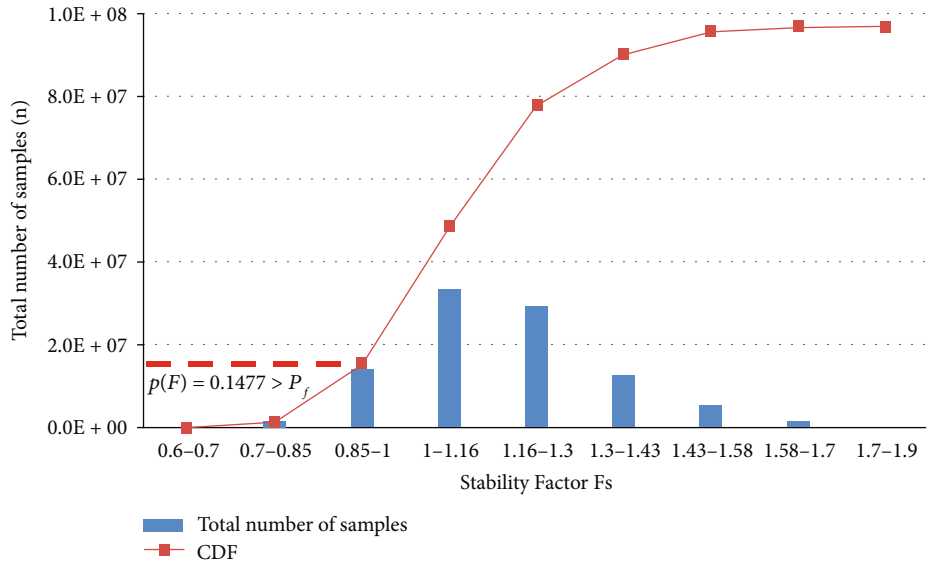

Figure 15: Statistical chart of slope stability coefficient based on the MCS method.

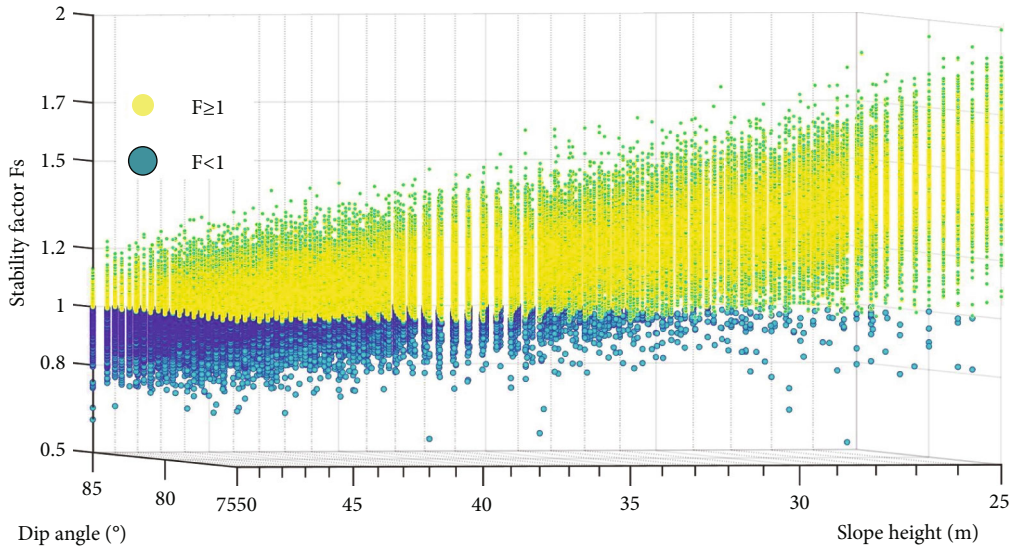

Figure 16: Statistical chart of stability coefficient under different combinations of slope height and slope angle.

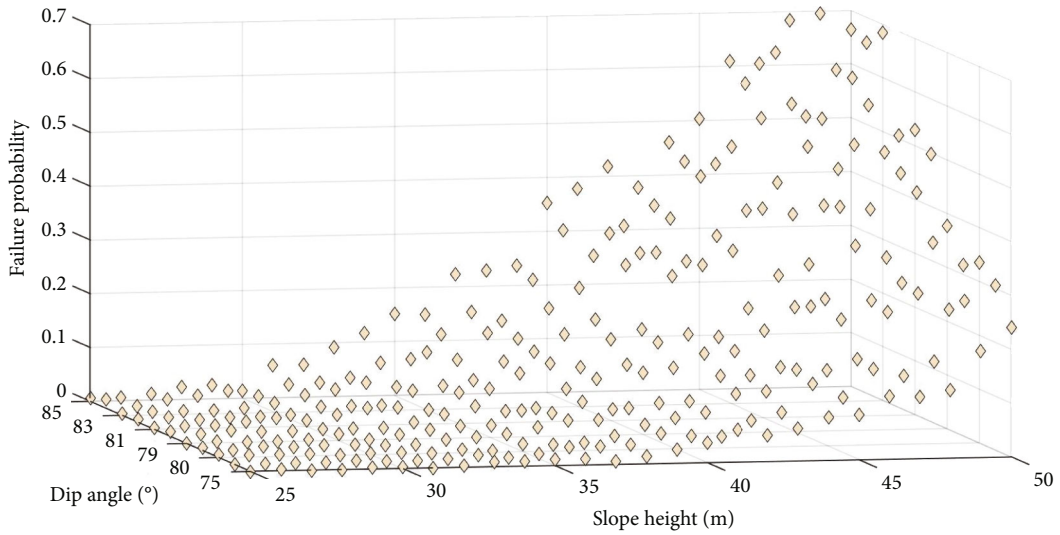

Figure 17: Statistical diagram of failure probability under different combinations of slope height and slope angle.

In order to reflect a specific failure probability value under 286 combinations of slope heights and angles, the failure probability value in a specific case was obtained through the calculation formula in literature [31–33] and the results are shown in Figure 17. It is observed that when the slope height is about 25 m, variations of the slope angle slightly affect the failure probability of the slope, indicating that until the slope height is small, it is the main influencing factor of stability. Moreover, when the slope height exceeds 33 m, the influence of the slope inclination on the stability gradually increases. The failure probability values of 249 combinations are obtained within the slope height range of 25~50 m. It is found that less than 87% of the combinations with different slope heights and angles are in the state of functional structure failure.

6. Conclusions

Based on the MCS method and the principle of limit equilibrium analysis, the cohesion c, internal friction angle φ, horizontal seismic acceleration coefficient $\boldsymbol{\alpha}$, and water-filling depth coefficient i in rock mass parameters are considered random variables, and the overall failure probability of slope and failure indices corresponding to different slope heights and slopes are calculated numerically. Accordingly, it is found that the target reliability index of the slope is far from the safe value within a certain range of slope height, and the slope is in a state of instability with a high probability. Aiming at performing timely measures, the main achievements can be summarized as follows:

(1) FCM-based clustering algorithm has a promising efficiency in analyzing a large number of random rock mass structural planes and can obtain ideal grouping results. Accordingly, this algorithm can provide a solid foundation for subsequent slope stability analysis and can be applied to determine the dominant structural planes of multiparameter rock mass structural planes

(2) The overall design service life of the slope has a high probability of functional failure, indicating that the overall slope is in an unstable state. Therefore, it is necessary to treat the slope in time. To this end, the Monte Carlo method is introduced to calculate the overall failure probability of the slope. The obtained results show that the overall failure probability of the slope is 0.1477, which is much higher than the target failure probability of the slope

(3) The combination of slope height and slope angle affects slope reliability. More specifically, as slope height and slope angle increase, more samples with a stability coefficient of less than 1 appear, and the failure probability of the slope increases, indicating that the slope is unstable. Until the slope height is small, it is the main influencing factor. However, when the slope height exceeds 33 m, the influence of the slope inclination on the stability gradually increases and 87% of the combinations with different slope heights and angles fail

Data Availability

The data used to support the findings of this study are included within the article.

Conflicts of Interest

The authors declare no conflict of interest, financial or otherwise.

Authors' Contributions

A. Fayou and Wan-cheng Pan have contributed equally to this work.

Acknowledgments

The authors acknowledge the National Natural Science Foundation of China (Grant: 42267020), the Project of High-quality Course Construction for Graduate Students of Yunnan Province in 2020(numerical simulation of geological engineering), and the Key Research and Development Program of Yunnan Province in 2022(202203 AC100003).

References

[1] K. Hirota, K. Konagai, K. Sassa, K. Dang, Y. Yoshinaga, and E. K. Wakita, "Landslides triggered by the West Japan heavy rain of July 2018, and geological and geomorphological features of soaked mountain slopes," *Landslides*, vol. 16, no. 1, pp. 189–194, 2019.

[2] Ö. Aydan, "Large rock slope failures induced by recent earthquakes," *Rock Mechanics and Rock Engineering*, vol. 49, no. 6, pp. 2503–2524, 2016.

[3] D. Lucas, R. Herzog, M. Iten et al., "Modelling of landslides in a scree slope induced by groundwater and rainfall," *International Journal of Physical Modelling in Geotechnics*, vol. 20, no. 4, pp. 177–197, 2020.

[4] J.-C. Chai and N. Miura, "Traffic-load-induced permanent deformation of road on soft subsoil," *Journal of Geotechnical and Geoenvironmental Engineering*, vol. 128, no. 11, pp. 907–916, 2002.

[5] N. K. Bhagat, A. K. Mishra, R. K. Singh, C. Sawmliana, and P. K. Singh, "Application of logistic regression, CART and random forest techniques in prediction of blast-induced slope failure during reconstruction of railway rock-cut slopes," *Engineering Failure Analysis*, vol. 137, article 106230, 2022.

[6] A. M. Youssef, A. H. El-Shater, M. H. El-Khashab, and B. A. El-Haddad, "Karst induced geo-hazards in Egypt: case study slope stability problems along some selected desert highways," in *International Congress and Exhibition, Sustainable Civil Infrastructures: Innovative Infrastructure Geotechnology*, pp. 149–164, Springer, Cham, 2017.

[7] D. Zai, R. Pang, B. Xu, Q. Fan, and M. Jing, "Slope system stability reliability analysis with multi-parameters using generalized probability density evolution method," *Bulletin of Engineering Geology and the Environment*, vol. 80, no. 11, pp. 8419–8431, 2021.

[8] S. Sasanian, A. Soroush, R. Jamshidi Chenari, and R. Shafipour Nourafshan, "Influence of geotechnical site investigation in horizontal plane on slope reliability," *Iranian Journal of Science and Technology, Transactions of Civil Engineering*, vol. 45, no. 3, pp. 1791–1803, 2021.

[9] A. Johari, A. Fazeli, and A. A. Javadi, "An investigation into application of jointly distributed random variables method in reliability assessment of rock slope stability," *Computers and Geotechnics*, vol. 47, pp. 42–47, 2013.

[10] A. Johari, M. Momeni, and A. A. Javadi, "An analytical solution for reliability assessment of pseudo-static stability of rock slopes using jointly distributed random variables method," *Iranian Journal of Science and Technology*, vol. 39, no. C2, pp. 351–363, 2015.

[11] A. Johari and A. Mehrabani Lari, "System probabilistic model of rock slope stability considering correlated failure modes," *Computers and Geotechnics*, vol. 81, pp. 26–38, 2017.

[12] W. Yu, Z. Cao, and S. K. Au, "Practical reliability analysis of slope stability by advanced Monte Carlo simulations in a spreadsheet," *Canadian Geotechnical Journal*, vol. 48, no. 1, pp. 162–172, 2011.

[13] A. E. Aladejare and V. O. Akeju, "Design and sensitivity analysis of rock slope using Monte Carlo simulation," *Geotechnical and Geological Engineering*, vol. 38, no. 1, pp. 573–585, 2020.

[14] L. Li and X. Chu, "Locating the multiple failure surfaces for slope stability using Monte Carlo technique," *Geotechnical and Geological Engineering*, vol. 34, no. 5, pp. 1475–1486, 2016.

[15] S. Li, H. B. Zhao, and Z. Ru, "Slope reliability analysis by updated support vector machine and Monte Carlo simulation," *Natural Hazards*, vol. 65, no. 1, pp. 707–722, 2013.

[16] A. Mahdiyar, M. Hasanipanah, D. J. Armaghani et al., "A Monte Carlo technique in safety assessment of slope under seismic condition," *Engineering with Computers*, vol. 33, no. 4, pp. 807–817, 2017.

[17] A. Alitabar, R. Noorzad, and A. Qolinia, "Evaluation of the instability risk of the dam slopes simulated with Monte Carlo method (case study: Alborz dam)," *Geotechnical and Geological Engineering*, vol. 39, no. 6, pp. 4237–4251, 2021.

[18] X. Tan, M. Shen, X. Hou, D. Li, and N. Hu, "Response surface method of reliability analysis and its application in slope stability analysis," *Geotechnical and Geological Engineering*, vol. 31, no. 4, pp. 1011–1025, 2013.

[19] X. C. Huang and X. P. Zhou, "Reliability analysis of a large-scale landslide using SOED-based RSM," *Environment and Earth Science*, vol. 76, no. 23, p. 794, 2017.

[20] X. Tan, X. Wang, X. Hu, M. F. Shen, and N. Hu, "Two methods for predicting reliability index and critical probabilistic slip surface of soil slopes," *Geotechnical and Geological Engineering*, vol. 34, no. 5, pp. 1283–1292, 2016.

[21] W. G. Zhang, F. S. Meng, F. Y. Chen, and H. L. Liu, "Effects of spatial variability of weak layer and seismic randomness on rock slope stability and reliability analysis," *Soil Dynamics and Earthquake Engineering*, vol. 146, no. 2021, article 106735, 2021.

[22] J. Q. Ma, G. J. Li, S. B. Li, and P. H. Xu, "Reliability analysis of embankment slope in Yaan-Luku expressway," *Applied Mechanics and Materials*, vol. 71-78, pp. 1360–1365, 2011.

[23] Z. J. Wu, S. L. Wang, and X. R. Ge, "Application of Latin hypercube sampling technique to slope reliability analysis," *Rock & Soil Mechanics*, vol. 31, no. 4, pp. 1047–1054, 2010.

[24] S. H. Jiang, D. Q. Li, C. B. Zhou et al., "Reliability analysis of unsaturated slope considering spatial variability," *Rock & Soil Mechanics*, vol. 35, no. 9, pp. 2569–2578, 2014.

[25] J. Zhou, M. Jiao, H. Xing, X. G. Yang, and Y. C. Yang, "A reliability analysis method for rock slope controlled by weak structural surface," *Geosciences Journal*, vol. 21, no. 3, pp. 453–467, 2017.

[26] S. K. Jha, "Effect of spatial variability of soil properties on slope reliability using random finite element and first order second moment methods," *Indian Geotechnical Journal*, vol. 45, no. 2, pp. 145–155, 2015.

[27] R. Kumar, P. Samui, and S. Kumari, "Reliability analysis of infinite slope using metamodels," *Geotechnical and Geological Engineering*, vol. 35, no. 3, pp. 1221–1230, 2017.

[28] H. S. B. Düzgün and A. Özdemir, "Landslide risk assessment and management by decision analytical procedure for Dereköy, Konya, Turkey," *Natural Hazards*, vol. 39, no. 2, pp. 245–263, 2006.

[29] J. C. Dunn, "Well-separated clusters and the optimal fuzzy partitions," *Journal of Cybernetics*, vol. 4, no. 1, pp. 95–104, 1974.

[30] Xiaoshu, *Study on Stability and Design Optimization of Jointed Rock Slope in Open-Pit Mine Based on Reliability Theory*, University of Science and Technology Beijing, 2016.

[31] A. H. S. Ang and W. H. Tang, *Probability Concepts in Engineering Planning and Design: Emphasis on Applications in Civil and Environmental Engineering*, Wiley, New York, 2007.

[32] X. Peng, D. Li, Z. Cao, X. S. Tang, and C. B. Zhou, "Reliability-based design approach of rock slopes using Monte Carlo simulation," *Chinese Journal of Rock Mechanics and Engineering*, vol. 35, no. S2, pp. 3794–3804, 2016.

[33] Y. Wang, S. K. Au, and F. H. Kulhawy, "Expanded reliability-based design approach for drilled shafts," *Journal of Geotechnical and Geo environmental Engineering*, vol. 137, no. 2, pp. 140–149, 2011.

[34] E. Hoek, *Practical rock engineering*, North Vancouver: Evert Hoek Consulting Engineer Inc, 2006.

[35] L. Wang, J. H. Hwang, C. H. Juang, and S. Atamturktur, "Reliability-based design of rock slopes – a new perspective on design robustness," *Engineering Geology*, vol. 154, pp. 56–63, 2013.